ELSEVIER

Polymer 42 (2001) 4375–4383

polymer

www.elsevier.nl/locate/polymer

Secondary dielectric β-relaxation in amorphous poly(ethylene terephthalate): combined thermally stimulated and isothermal depolarization current investigations

J. Ménégotto, Ph. Demont*, C. Lacabanne

Laboratoire de Physique des Polymères, L2P-CIRIMAT UMR 5085, Université P. Sabatier, 118 rte de Narbonne, 31062 Toulouse Cedex, France

Received 9 May 2000; received in revised form 27 September 2000; accepted 28 September 2000

Abstract

The complex β dielectric relaxation process in amorphous poly(ethylene terephthalate) (PET) is investigated by thermally stimulated depolarization currents (TSDC) and isothermal depolarization currents (IDC) techniques. TSDC and IDC data are analyzed in the framework of the Ngai coupling model in the [−150; −40°C] temperature range using the Marchal method and involving a Kohlrausch–Williams–Watts (KWW) functional form of the polarization time decay. The temperature dependence of the characteristic τ_{KWW} relaxation time and of the β_{KWW} stretching parameter of the KWW relaxation function derived from both depolarization current methods for the β relaxation of PET are determined and then compared. The very good agreement observed between the two sets of experimental stretching parameters determined by TSDC and IDC confirms the high potentiality of the TSDC technique to study complex relaxation processes as such as the β relaxation of PET. The two different overlapped relaxation processes involved in the β relaxation have been confirmed throughout the determination of two different temperature behaviors of the β_{KWW} parameter. Each process of complex β relaxation is characterized by a low and nearly temperature-independent KWW stretching parameter. We show that the β_{KWW} value of the high-temperature component, involving phenyl group motions, is slightly lower than the one corresponding to the low-temperature process assigned to the motions of carbonyl groups. © 2001 Elsevier Science Ltd. All rights reserved.

Keywords: Thermally stimulated depolarization currents; Isothermal depolarization currents; Poly(ethylene terephthalate)

1. Introduction

Amorphous polymers are well known to exhibit very broad, non-Debye like, dielectric and mechanical relaxation processes commonly referred as α and β relaxations.

In the time domain, the α relaxation which is generally associated with the mechanical or dielectric manifestation of the “dynamic glass transition” of polymer, can be well described by means of a stretched exponential or Kohlrausch–Williams–Watts [1] (KWW) function:

$$\phi(t) = \exp\left[-\left(\frac{t}{\tau_{KWW}}\right)^{\beta_{KWW}}\right] \quad (1)$$

where $\beta_{KWW} \in]0,1]$ is the stretching parameter which takes into account the complexity of the response and τ_{KWW} is the characteristic relaxation time. On the other hand, in the frequency domain, the dielectric α relaxation process is usually well described by the empirical Havriliak–Negami [2] (HN) equation:

$$\epsilon^*(\omega) = \epsilon_\infty + \frac{\epsilon_s - \epsilon_\infty}{[1 + (i\omega\tau_{HN})^{\alpha_{HN}}]^{\gamma_{HN}}} \quad (2)$$

where ϵ_s and ϵ_∞ are, respectively, the relaxed ($\omega = 0$) and unrelaxed ($\omega = \infty$) dielectric constants, τ_{HN} is the characteristic relaxation time and α_{HN} and γ_{HN}, $[0 < (\alpha_{HN}, \gamma_{HN}) < 1]$ are the shape parameters which describe, respectively, the symmetrical and asymmetrical broadening of relaxation curves [2,3]. A direct analytical connection between these two different phenomenological equations, particularly suitable to describe complex responses recorded in frequency or time domain, is not yet available in spite of great efforts of many authors. Nevertheless, based on rigorous experimental analyses, an empirical relationship between the KWW stretching parameter and the HN shape parameters has been proposed by Alvarez et al. [4] for α relaxation:

$$(\alpha_{HN}\gamma_{HN}) = (\beta_{KWW})^{1.23} \quad (3)$$

In polymers, the β relaxation, associated with localized

---

* Corresponding author. Tel.: +33-5-61556538; fax: +33-5-61556221.
E-mail address: demont@cict.fr (Ph. Demont).

0032-3861/01/$ - see front matter © 2001 Elsevier Science Ltd. All rights reserved.
PII: S0032-3861(00)00732-1

motions of the totality or a part of constitutive units of the macromolecule, involves broader distribution of relaxation times than an α relaxation. This large relaxation time distribution yields broad spectra which are often described in the frequency domain by the symmetrical Cole and Cole function [5]. This empirical function corresponds to the special case of the HN equation with $\gamma_{\rm HN} = 1$. Nevertheless, broadband dielectric spectroscopy which easily covers 12 decades in frequency, shows the asymmetrical nature of secondary dielectric relaxation process in complex systems. For example, the very broad available frequency range allowed Casalini et al. [6] to take into account, by means of an HN equation, the departure from the symmetric shape of the dielectric β relaxation in diglycidyl ether of bisphenol-A system. Bergman et al. [7,8] have shown that the β relaxation of syndiotactic poly(methyl methacrylate) (PMMA) is asymmetric and cannot be described by a Cole–Cole function, even at sufficiently low temperatures where the α and β processes are well separated in frequency. To study dynamics of the β process in PMMA, KWW and HN functions have been used by Bergman et al. [7,8] to fit dielectric data in time and frequency domains, respectively. In the case of polymers without side groups on their backbone, as poly(ethylene terephthalate) (PET), the secondary dielectric relaxation process has also been described in the past by a Cole–Cole equation [9,10]. Nevertheless, recent dielectric and mechanical investigations [11] carried out on PET reveal, through the broadness and asymmetry of dielectric loss curves, the complex nature of the secondary relaxation. Hofmann et al. [12] and Richert [13] used an HN relaxation function to describe the β process of PET over a very broad frequency range (10^{-2}–10^{9} Hz). They indicate that the HN asymmetrical shape parameter $\gamma_{\rm HN}$ changes from 0.97 to 0.5 when the temperature is lowered from 363 to 343 K [13]. Considering the relationship among the HN and KWW parameters allowed for the α relaxation [see Eq. (3)] and conceivable for the β relaxation, the KWW relaxation function can also be adopted to analyze the behavior of the β process in PET in the time domain.

Illers and Breuer [14] interpreted the asymmetric character of the secondary relaxation of PET in terms of overlapped processes. More recently, Maxwell et al. [11,15], using nuclear magnetic resonance (NMR) and dielectric and mechanical spectroscopies, have shown that the β relaxation peak in PET consists of two different relaxation processes. By comparing results obtained for PET and PET with additive blends, the higher-temperature process has been associated with the motions of phenyl rings, whereas the lower-temperature process has been addressed to the carbonyl motions [15].

In spite of these results, further effort must be undertaken to specify the origin of the non-exponentiality or asymmetry of the secondary relaxation mode in PET, observed in the time or in the frequency domain. Indeed, this complex response could arise from either an overlap of two symmetric processes or an overlap of two complex and asymmetric processes.

The purpose of this dielectric investigation is to determine the $\beta_{\rm KWW}$ parameter associated with the β relaxation process of PET and to obtain new insight about the dynamics of the overlapped processes. Different experimental techniques are generally used to obtain information about the dynamics of glass-forming materials, including dielectric spectroscopy [11,12,16–19], isothermal depolarization currents (IDC) [17,18,20–22], dynamic mechanical measurements [11,23–27], dynamic light and neutron scattering [27–32] and NMR [15,33–34]. However, in order to enhance the resolution of the overlapped relaxation processes involved in the β relaxation of PET, the technique of thermally stimulated depolarization currents (TSDC), has been used. Indeed, an important feature of TSDC is its low equivalent frequency. In a recent paper [35] we have shown the high-resolution capability of TSDC and the good agreement between results obtained by TSDC and dynamic dielectric spectroscopy on the secondary relaxation of PET. In order to check the KWW parameters obtained from TSDC data in the low-temperature and -frequency ranges, the IDC technique has also been performed.

To describe dynamical processes in complex systems, Ngai [36–40] proposes, in the coupling model (CM), a theoretical meaning of the KWW function. In order to explain the physical basis of the stretched exponential function, the CM assumes the existence of a coupling of the primitive or isolated segmental relaxation processes to their complex surroundings. This coupling would be responsible for the non-Debye relaxation behavior of the complex systems. The degree of coupling, characterized by the parameter n in the CM model, is related to the KWW parameter by $\beta_{\rm KWW} = 1 - n$.

The aim of this study is the determination of the KWW parameters in the secondary relaxation of amorphous PET by using IDC and TSDC techniques. The analysis of TSDC and IDC data has been carried out by means of the Marchal procedure [41–44] which uses the CM of Ngai as an analytical support.

2. Experiments

2.1. Materials

The investigated PET samples were supplied by Dupont de Nemours (Luxembourg) in amorphous sheets form of 350 mm thickness. The glass transition temperature $T_{\rm g} = 74$°C was determined by differential scanning calorimetry using a heating rate of 10°C $\rm min^{-1}$. The cold-crystallization and melting temperatures were observed at 133 and 255°C, respectively. The difference between cold-crystallization and melting peaks areas, normalized to the heat of melting $\Delta H_{\rm m} = 140\ {\rm J\ g^{-1}}$ for 100% crystalline PET, yields no measurable amount of crystallinity ($\chi_{\rm c} < 3\%$). The onset of the crystallization was estimated at 94°C. In order to avoid the cold-crystallization of the amorphous PET during

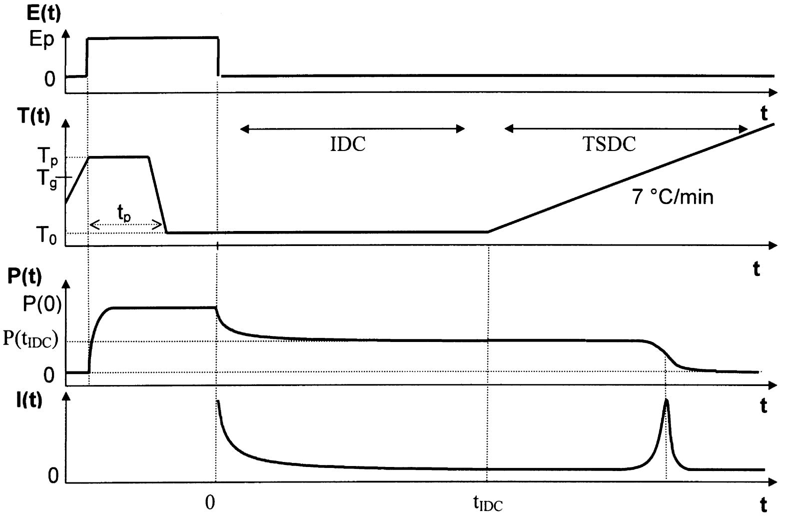

Fig. 1. Principle of the IDC method followed by a TSDC procedure. Schematic time evolution of the different parameters involved in an IDC experiment.

TSDC experiment, the upper measurement temperature did not exceed 90°C.

2.2. Thermally stimulated depolarization currents

TSDC measurements were carried out with a dielectric apparatus developed in our laboratory from the concept outlined by Bucci and Fieschi [45] and described elsewhere [46,47]. In order to obtain a TSDC spectra the sample was polarized by a static electric field, $E_p = 10^3\ \mathrm{V\ mm^{-1}}$, at the polarization temperature $T_p = 85°\mathrm{C}$ during a time $t_p =$ 2 min, which was enough long to attain the equilibrium polarization ($t_p > \tau(T_p)$). The sample was then quenched, with the polarization field still on, from T_p to the freezing temperature $T_0 = -185°\mathrm{C}$ where the orientation polarization $P(T_p)$ was frozen-in. At T_0, the field was cut off and the sample was short-circuited for a time $t_{cc} = 1$ min to remove fast relaxing surface charges and stabilize the sample temperature. The depolarization current $I(T)$ was then recorded through a Keithley 642 electrometer as the temperature increased from T_0 up to T_f. T_f was the final temperature such that $T_p < T_f < 90°\mathrm{C}$. The temperature was increased with different linear heating rates: 3, 5, 7, 9 and 11°C min^{-1}.

2.3. Isothermal depolarization current

In the first steps of the experimental procedure, the IDC technique is similar to the TSDC method. The sample was polarized by a static electric field $E_p = 10^3\ \mathrm{V\ mm^{-1}}$ at $T_p =$ 85°C for a time $t_p = 2$ min. Then the sample was quenched from T_p to the isothermal temperature measurement T. When the thermal equilibrium at temperature T was reached, the field was removed at a time set as origin of time. Afterwards, the isothermal depolarization current was recorded as a function of time up to $t_{IDC} = 900$ s, the time at which the signal to noise ratio increased in a significant manner. The recorded current corresponds to the return to equilibrium of the dipole polarization.

However, in order to recover slow relaxation processes and to obtain the remaining polarization in a reasonable interval of time, the temperature is increased at 7°C min^{-1} after the time t_{IDC} from T up to T_f as an usual final TSDC scan. This added depolarization procedure, introduced by Marchal [41–44], is essential for the determination of the stretching parameter β_{KWW}. The principle of the IDC method is described in Fig. 1 where the static electric field E_p, the sample temperature T, the orientation polarization P and the depolarization current I have been displayed as a function of time.

The IDC procedure developed in the present work is slightly different from the one used by Alegria et al. [17,18,20–22]. Indeed, these authors polarized the sample at the isothermal depolarization temperature during a time t_p long enough to achieve the equilibrium polarization. Nevertheless, due to the intrinsic structural instability of the glassy state ($T < T_g$), their polarization time t_p could modify the state of the system and comparison of the IDC results obtained at different temperatures could be hazardous if the structure of the material is changing. In order to overcome this problem, Alegria et al. introduce an annealing time $t_a(T)$ which was added to t_p. This annealing time would produce the same relaxed enthalpy or configuration state of the sample at the beginning of the depolarization process for each investigated temperature. The annealing time t_a has been previously determined by differential scanning calorimetry study. It was dependent on the measurement temperature.

In contrast to Alegria et al., the IDC and TSDC methods use the same conditions of application of the static electric field. Since $T_p > T_g$, the thermal history of the sample is removed before each experiment and the equilibrium polarization is reached. When the sample is quenched from T_p to T in the IDC test or to T_0 in the TSDC experiment, the

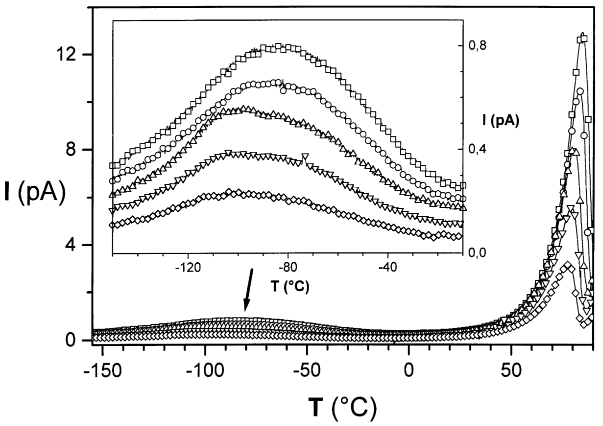

Fig. 2. TSDC spectra of amorphous PET obtained between −160 and 85°C by using five heating rates: (□) 11, (○) 9, (△) 7, (▽) 5 and (◇) 3°C min^{-1}. The inset shows an enlargement of the β relaxation. The polarization temperature is $T_p = 85$°C.

system falls in an out-of equilibrium state in the same way for all the experiments, and an identical structural state is reasonably reached at the beginning of the IDC or TSDC measurements. Hence the IDC results, obtained at different temperatures T, can be compared to each other and to the TSDC results. Unlike the method of Alegria, the present procedure avoids taking into account physical aging before the $I(t)$ decay measurements and allows the comparison between TSDC and IDC results.

3. Coupling model

The CM of Ngai is widely used to describe dynamical processes in a great number of materials [16,36–40]. This model establishes a fundamental relationship between the macroscopic and the microscopic levels of a relaxation property which provides an interesting way to understand the molecular structure of condensed matter throughout the study of the relaxation time behavior.

The CM assumes the existence of primitive species which relax with a time-independent relaxation time τ_0. However, the complexity of systems implies a physical coupling between these primitive or isolated species and their environment. This coupling occurs after the temperature-independent crossover time t_c (in polymers $t_c = 2 \times 10^{-12}$ s [29]). The interactions responsible for this coupling slow down the relaxation rate of primitive species with the result that the relaxation time becomes time dependent. Ngai suggested the following time dependence for the relaxation time:

$$\tau(t) = \tau_0 \qquad t < t_c \tag{4}$$

$$\tau(t) = \tau_0 \left(\frac{t}{t_c}\right)^n \qquad t > t_c \tag{5}$$

where n is a parameter describing the coupling strength between the primitive species and their environment. These equations involve, in the case of the dielectric relaxation, the following expressions for the orientation polarization P taken as the relaxing quantity in our study:

$$P(t) = P(0)\exp\left(-\frac{t}{\tau_0}\right) \qquad t < t_c \tag{6}$$

$$P(t) = P(0)\exp\left(-\left(\frac{t}{\tau^*}\right)^{1-n}\right) \qquad t > t_c \tag{7}$$

where $P(0)$ is the initial or unrelaxed polarization value.

Eq. (7) of the CM leads to the well-known KWW function, with $\beta_{\mathrm{KWW}} = 1 - n$ and $\tau_{\mathrm{KWW}} = \tau^*$. The relaxation time τ^* is the macroscopic relaxation time closely related to the microscopic relaxation time τ_0 by Eq. (8):

$$\tau^* = [(1-n)t_c^{-n}\tau_0]^{1/(1-n)} \tag{8}$$

according to the continuity of the relaxation time $\tau(t)$ at $t = t_c$ (see Eqs. (4) and (5)). Nevertheless, recent developments of the CM [39] suggest replacing Eq. (8) by Eq. (9) arising from the continuity of the polarization $P(t)$ at $t = t_c$ (Eqs. (6) and (7)).

$$\tau^*(T) = [t_c^{-n}\tau_0(T)]^{1/(1-n)} = [t_c^{\beta_{\mathrm{KWW}}-1}\tau_0(T)]^{1/\beta_{\mathrm{KWW}}} \tag{9}$$

Based on better physical conditions this last equation will be used in this work to analyze the TSDC and IDC data.

As generally observed in glass-forming materials, the dielectric or mechanical macroscopic relaxation time of secondary β relaxation exhibits an Arrhenius temperature dependence:

$$\tau^*(T) = \tau^*_\infty \exp\left(\frac{E^*_A}{k_B T}\right) \tag{10}$$

where E^*_A and τ^*_∞ are, respectively, the apparent activation energy and the pre-exponential factor of τ^*.

When a slight temperature dependence of the β_{KWW} and t_c parameters is observed, from Eqs. (8) and (9) a similar temperature behavior for the τ_0 primitive relaxation time can be deduced:

$$\tau_0(T) = \tau_\infty \exp\left(\frac{E_A}{k_B T}\right) \tag{11}$$

where E_A and τ_∞ are the activation energy and the pre-exponential factor of primitive relaxation time, respectively.

Then Eqs. (8) and (9) allow a direct relationship between the apparent activation energy, E^*_A, of the macroscopic relaxation process and the activation energy, E_A, of the associated primitive motions to be obtained, namely:

$$E^*_A = \frac{E_A}{\beta_{\mathrm{KWW}}} \tag{12}$$

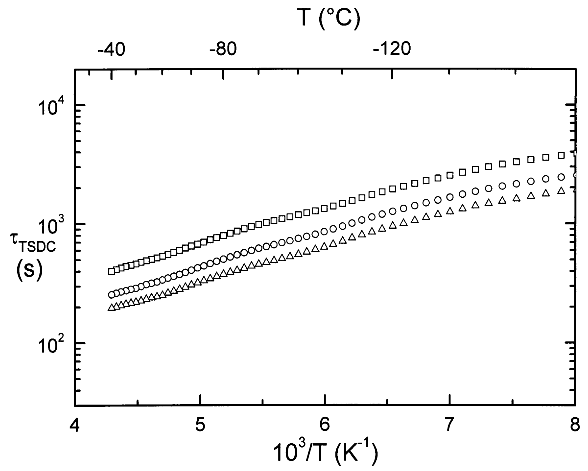

Fig. 3. Temperature dependence of the effective relaxation time determined following the TSDC method limited to the three heating rates: (□) 3, (○) 5 and (△) 7°C min^{-1}.

4. Results

4.1. TSDC analysis

The TSDC spectra recorded at different heating rates (3, 5, 7, 9 and 11°C min^{-1}) in PET samples, polarized at 85°C, are displayed in Fig. 2. Two different relaxation processes are resolved. On the one hand, the most intensive and narrower TSDC peak, observed at about 74°C and labeled the α process, has been addressed, in accordance with the literature [48–50] to the dielectric manifestation of the glass transition. On the other hand, at lower temperatures, the weaker and broader peak centered about −90°C has been associated to the β secondary relaxation process [35,48]. The inset in Fig. 2 enlarges the low-temperature range of the β relaxation.

As expected, we note that an increase of the heating rate leads to a shift of each relaxation processes towards higher temperatures with, at the same time, a decrease of the distance between the α and β relaxation peaks. However, the area under each TSDC curve, normalized to the heating rate, remains the same. These observations are compatible with the increase of the TSDC equivalent frequency with the heating rate [51].

The aim of this article is to study the secondary relaxation of PET, so we do not concentrate on the α process which will be analyzed elsewhere. As it can be seen in the inset of Fig. 2, when the equivalent frequency of the TSDC technique is lowered by decreasing the heating rate, the β peak observed at higher frequency (higher heating rates) splits into two processes, named β_1 and β_2 in the order of decreasing temperature. This splitting of the two overlapped processes has been shown to be consistent with dynamic dielectric results exposed in a previous paper [35] where a discussion about the non-observation by Maxwell et al. [11] of these two dielectric processes has been done. After considerations of the NMR and mechanical results of Refs. [11,15] and our dielectric observations, we conclude that whereas the lower-temperature relaxation process could be associated with the carbonyl motions, the higher-temperature process could correspond to the motions of phenyl rings.

In order to analyze the complexity of the two overlapped secondary relaxations, only TSDC spectra recorded with the lower heating rates 3, 5 and 7°C min^{-1} are considered afterwards. Indeed, only these spectra are characteristic of the bimodal nature of the β relaxation of PET.

The TSDC data analysis performed by using the Marchal method in the framework of the CM is based on the calculation of the effective relaxation time $\tau_{TSDC}(T)$. In a TSDC experiment, this relaxation time is obtained using the Bucci–Fieschi–Guidi [45] equation:

$$\tau_{TSDC}(T) = \frac{SP(T)}{I(T)} = \frac{1}{q}\frac{\int_T^{T_f} I(T')\mathrm{d}T'}{I(T)} \tag{13}$$

where S is the sample area, $P(T)$ and $I(T)$ are the polarization and depolarization current at temperature T, respectively, q is the heating rate and T_f is the final temperature of the recorded TSDC spectrum.

The temperature dependence of the effective relaxation time τ_{TSDC} is reported in Fig. 3 for the three different heating rates 3, 5 and 7°C min^{-1}. As expected, in respect to the TSDC equivalent frequency change with heating rate [51], we note that for all temperatures, the τ_{TSDC} relaxation time decreases with increasing heating rate. This effective relaxation time, which corresponds to the time necessary to the return to the equilibrium state of selected species coupled with their environment, has been assumed to be the relaxation time $\tau(t)$ introduced by Ngai (see Eqs. (4) and (5)). Moreover, using the very low equivalent frequency of the TSDC measurements we can also assumed that the experimental time is much longer than the crossover time t_c. So Eq. (5) must be checked by the τ_{TSDC} effective relaxation time where the substitution of the time t by $[(T - T_0)/q_i)]$ for a linear heating rate q_i leads to:

$$\tau_{TSDCi}(T) = \tau_i(T) = \tau_0(T)t_c^{\beta_{KWW}-1}\left(\frac{T-T_0}{q_i}\right)^{1-\beta_{KWW}} \tag{14}$$

With the heating rates used, we assume that PET samples stay in an iso-configurational state, or in other words that no physical aging occurs during the TSDC temperature scan. So the three parameters τ_0, t_c and β_{KWW} can be considered as time independent. The different $I(T)$ curves are obtained by means of a same TSDC thermal procedure and with close heating rates. We can also assume that these parameters are heating rate independent. Then β_{KWW} can be calculated from Eq. (14) throughout the ratio between relaxation times determined using two different linear

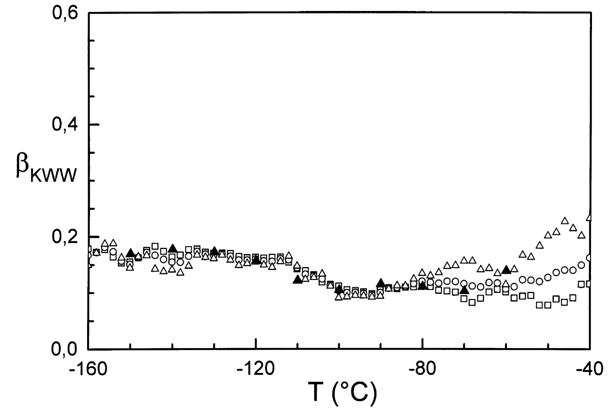

Fig. 4. Temperature dependence of the β_{KWW} parameters determined from TSDC experiments (open symbols) and from IDC experiments (solids symbols) for the β relaxation in amorphous PET. The different open symbols correspond to the different β_{KWW} values obtained from the three different heating rates according to Eq. (15).

heating rates q_i and q_j:

$$\beta_{KWW}^{i,j}(T) = 1 - \frac{\ln\left(\frac{\tau_i(T)}{\tau_j(T)}\right)}{\ln\left(\frac{q_j}{q_i}\right)} \tag{15}$$

Using the three different linear heating rates 3, 5 and 7°C min^{-1}, three temperature dependencies of the $\beta_{KWW}^{i,j}(T)$ parameter have been calculated using this method, reported in the literature as the Marchal procedure [41–44]. The $\beta_{KWW}^{i,j}(T)$ values obtained for the secondary relaxation of PET are plotted in Fig. 4 as open symbols. Excepted above −60°C where a scattering of $\beta_{KWW}^{i,j}(T)$ values is observed, we note that the $\beta_{KWW}^{i,j}(T)$ parameter is heating rate independent.

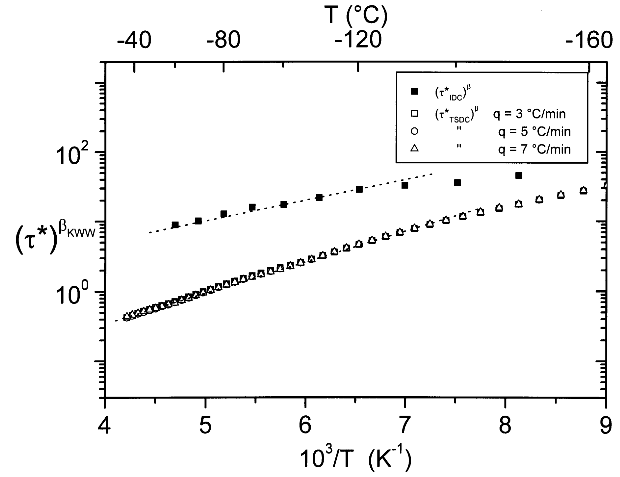

Fig. 5. Representation of $(\tau^*)^{\beta_{KWW}}$ parameters determined from TSDC (open symbols) and IDC (solid symbols) experiments versus reciprocal temperature. The different open symbols correspond to the different $(\tau^*)^{\beta_{KWW}}$ values obtained from the three different heating rates. Dashed lines show linear fits according to Eq. (16) for TSDC data and Eq. (22) for IDC data.

In order to determine the activation energy E_A of the primitive species involved in the β relaxation process, Eq. (14) can be rewritten using Eqs. (9) and (11) as:

$$\ln(\tau_{TSDC}(T)) + (\beta_{KWW} - 1)\ln\left(\frac{T - T_0}{q}\right) = \ln[(\tau^*_{TSDC})^{\beta_{KWW}}]$$

$$= \frac{E_A}{k_B T} + \Sigma \tag{16}$$

where

$$\Sigma \equiv \ln \tau_\infty + (\beta_{KWW} - 1)\ln t_c \tag{17}$$

Fig. 5 shows, in a semi-logarithmic scale versus reciprocal temperature, the $(\tau^*_{TSC})^{\beta_{KWW}}$ values calculated using the right term of Eq. (16). A similar Arrhenius behavior is observed for the three curves associated with the different heating rates used in the [−135°C; −40°C] temperature range where the β TSDC peak occurs. This representation, which corresponds to a heating rate normalization of the τ_{TSDC} effective relaxation times displayed in Fig. 3, leads to the superposition of $(\tau^*_{TSC})^{\beta_{KWW}}$ curves obtained with different q_i. This feature confirms the previously determined β_{KWW} values. A linear fit of the temperature dependence of the three $(\tau^*_{TSC})^{\beta_{KWW}}$ curves allows to extract, with respect to the left term of Eq. (16), the heating rate-independent activation energy of primitive species, $E_A = 8.5 \pm 0.1$ kJ mol^{-1}, and the intercept, $\Sigma = -5.1 \pm 0.3$.

From the average value $\overline{\beta_{KWW}} = 0.150 \pm 0.03$ of the stretched parameter determined by a linear fit of all $\beta_{KWW}^{i,j}(T)$ curves in the [−160; −40°C] temperature range (see Fig. 4) and using $t_c = 2$ ps [29] in the expression of Σ, the pre-exponential factor of the primitive species has been evaluated as $\tau_\infty = 7 \times 10^{-13}$ s.

Moreover, with $\overline{\beta_{KWW}} = 0.150 \pm 0.03$ and $E_A = 8.5 \pm 0.1$ kJ mol^{-1}, the activation energy $E_A^* = 57 \pm 12$ kJ mol^{-1} of the macroscopic relaxation time, τ^*_{TSDC}, has been determined using Eq. (12).

4.2. IDC analysis

Results obtained on PET samples following our IDC procedure are shown in Fig. 6a and b. IDC spectra of the PET sample polarized at $T_p = 85$°C have been recorded in the [−150; −60°C] temperature range in steps of 10°C as time swept the [0; 900 s] time domain and presented in Fig. 6a. The semi-logarithmic representation of these spectra allows the observation, in the time domain, the non-exponential decay of depolarization current in the low-temperature range corresponding to the β relaxation mode of PET. This point confirms the suitability of the KWW description of the PET dielectric behavior in this temperature range. The TSDC spectra which are characteristic of the remaining polarization after each isothermal depolarization are displayed in Fig. 6b. The TSDC heating procedure begins

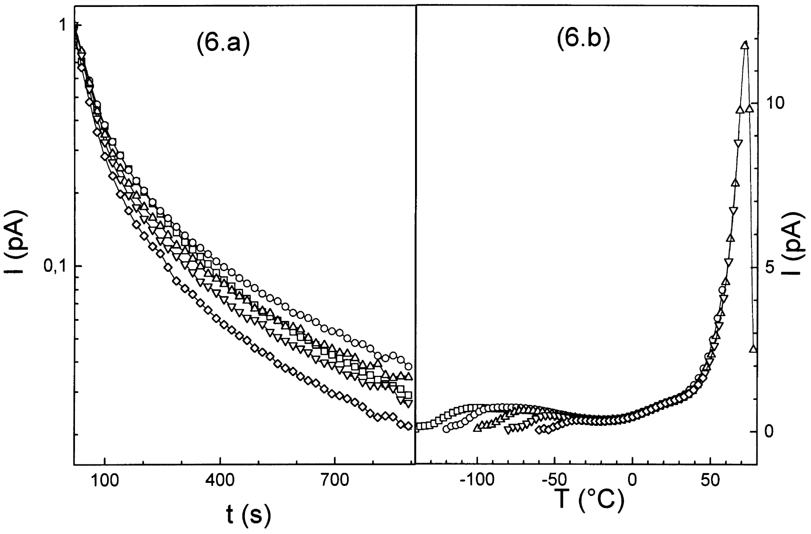

Fig. 6. (a) Isothermal decay of IDC for several temperatures. For clarity only data recorded at the following temperatures are shown: (□) −140, (○) −120, (△) −100, (▽) −80 and (◇) −60°C. (b) TSDC spectra obtained immediately after the IDC measurements mentioned above. For symbols see (a).

at the IDC temperature measurement with a rate of 7°C min^{-1} and ends at $T_f > T_g$. These spectra reveal an unmodified relaxation peak, located about 74°C, associated with the previously observed α relaxation. At low temperatures, the weak and broad TSDC peak arises from the disorientation of the unrelaxed dipoles during IDC measurements and is involved in the β relaxation process.

The fact that the sum of areas under both the IDC curve and its associated TSDC spectrum is constant proves that the initial polarization $P(0)$ is the same for all the IDC experiments.

As previously underlined, the main difficulty lies in the estimation of the unrelaxed polarization $P(t)$ over an experimental time range limited to t_{IDC}. This is the reason of the use of the TSDC procedure at the end of time t_{IDC}. The unrelaxed polarization at time t between 0 and t_{IDC} can be expressed as:

$$P(t) = P_{IDC}(t) + P_{TSDC} \tag{18}$$

where

$$P_{IDC}(t) = \frac{1}{S}\int_t^{t_{IDC}} I_{IDC}(t')\mathrm{d}t' \tag{19}$$

is the time-dependent unrelaxed polarization available from the area under the IDC curve, and

$$P_{TSDC} = \frac{1}{qS}\int_T^{T_f} I_{TSDC}(T')\mathrm{d}T' \tag{20}$$

is the unrelaxed polarization after the IDC measurement and is only available during the TSDC procedure.

The effective relaxation time is then determined over the [0; t_{IDC}] time range according to Eq. (21):

$$\tau_{IDC}(t) = S\frac{P_{IDC}(t) + P_{TSDC}}{I_{IDC}(t)} \tag{21}$$

In the framework of the CM, the time dependence of the effective relaxation time, $\tau_{IDC}(t)$, obeys Eq. (5) and can be expressed as:

$$\ln(\tau_{IDC}(t)) = (1 - \beta_{KWW})\ln(t) + \Sigma' \tag{22}$$

with

$$\Sigma' \equiv \ln(\tau_0 t_c^{\beta_{KWW}-1}) \tag{23}$$

The time dependence of the effective relaxation time has been reported on a log–log scale in Fig. 7 for all the investigated temperatures. As expected the relaxation time decreases with increasing temperature at any time. From a linear regression of the linear part observed in the [60; 900 s] time domain, the β_{KWW} and Σ' parameters have been determined for each temperature using Eq. (22).

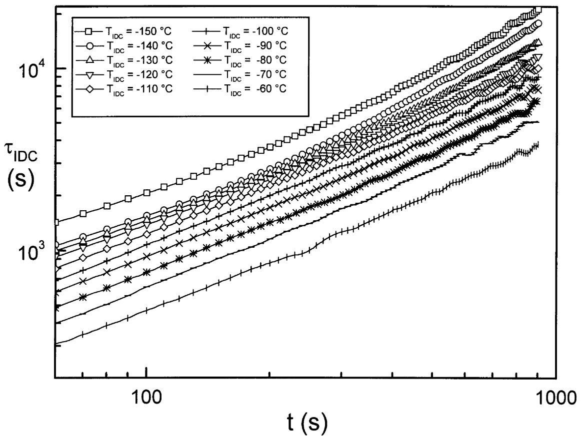

Fig. 7. Time dependence of the IDC experimental relaxation time at several temperatures using IDC and TSDC procedures according to Eq. (21).

Indeed, the slope of the $\ln(\tau_{\mathrm{IDC}}(t))$ versus $\ln(t)$ curves gives an accurate determination of the β_{KWW} coupling parameter and Σ' represents the intercept of the linear part at $t = 0$. To compare the IDC and TSDC β_{KWW} parameters, we have also reported the temperature dependence of IDC β_{KWW} parameter in Fig. 4.

In order to determine the activation energy of primitive species involved in the β relaxation process of PET, the $(\tau^*_{\mathrm{IDC}})^{\beta_{\mathrm{KWW}}}$ parameter has been calculated at each isothermal temperature from a combination of Eqs. (9) and (23) and using the Σ' values. In the Arrhenius diagram of Fig. 5, the respective temperature dependencies of $(\tau^*_{\mathrm{IDC}})^{\beta_{\mathrm{KWW}}}$ and $(\tau^*_{\mathrm{TSDC}})^{\beta_{\mathrm{KWW}}}$ have been compared. From a non-linear fit of the temperature dependence of the $(\tau^*_{\mathrm{IDC}})^{\beta_{\mathrm{KWW}}}$ relaxation time by Eq. (16), the values of the microscopic activation energy is determined: $E_{\mathrm{A(IDC)}} = 5.5 \pm 0.3\ \mathrm{kJ\ mol^{-1}}$. Such a value is lower than the one obtained from the TSDC data ($8.5\ \mathrm{kJ\ mol^{-1}}$). Assuming that $E_{\mathrm{A(IDC)}} = 5.5 \pm 0.3\ \mathrm{kJ\ mol^{-1}}$ and taking $\overline{\beta_{\mathrm{KWW}}} = 0.15$, which is the average value of stretched parameter β_{KWW} over the β relaxation temperature range, the macroscopic activation energy of the dielectric secondary relaxation of PET is calculated, according to Eq. (12): $E^*_{\mathrm{A(IDC)}} \approx 40 \pm 2\ \mathrm{kJ\ mol^{-1}}$.

5. Discussion

Fig. 4 shows the superposition of the different temperature dependencies of coupling parameters obtained from different heating rate pairs in TSDC experiments. We note that in the $[-160, -80°\mathrm{C}]$ temperature range, the values of β_{KWW} are heating rate independent. This result is in agreement with the assumption of an iso-configurational state of sample during the depolarization current recording at the different controlled heating rates including the lowest one used ($3°\mathrm{C\ min^{-1}}$). Time and heating rate-independent kinetic parameters, E_{A}, τ_∞ and E^*_{A} of dielectric β relaxation in PET have been determined from the TSDC data.

In the entire investigated temperature range of the β relaxation of PET, same temperature behaviors and same values of the β_{KWW} parameter are obtained from the TSDC and IDC data as shown in Fig. 4 by means of the superposition of solid and open symbols.

As a first approach of the β_{KWW} temperature dependence, we can consider $\beta_{\mathrm{KWW}}(T)$ weakly temperature dependent and well characterized, in the whole investigated temperature range, by its mean value $\overline{\beta_{\mathrm{KWW}}} = 0.15$. This consideration allows to determine $(\tau^*)^{\beta_{\mathrm{KWW}}}$, from TSDC and IDC measurements. $(\tau^*)^{\beta_{\mathrm{KWW}}}$ is associated with the dynamic of primitive species involved in the secondary β relaxation of PET (see Fig. 5). The activation energy of primitive species E_{A} and the macroscopic activation energy E^*_{A} have been obtained from $\overline{\beta_{\mathrm{KWW}}} = 0.15$ and through the study of the $(\tau^*)^{\beta_{\mathrm{KWW}}}$ temperature dependence. Weak differences between the TSDC and IDC results about the $(\tau^*)^{\beta_{\mathrm{KWW}}}$ values are noted (less than one decade). The primitive and macroscopic activation energy are, respectively, $E_{\mathrm{A}} = 8.5\ \mathrm{kJ\ mol^{-1}}$ and $E^*_{\mathrm{A}} = 5.7\ \mathrm{kJ\ mol^{-1}}$ obtained from TSDC and $E_{\mathrm{A}} = 5.5\ \mathrm{kJ\ mol^{-1}}$ and $E^*_{\mathrm{A}} = 40\ \mathrm{kJ\ mol^{-1}}$ obtained from IDC. These weak differences are not yet precisely understood but it seems that they arise only from the limited IDC experimental time range. Indeed, the macroscopic activation energy found in the literature for the β process of PET and determined by dynamic dielectric ($56\ \mathrm{kJ\ mol^{-1}}$ [11] or $66\ \mathrm{kJ\ mol^{-1}}$ [52]) or mechanical ($62\ \mathrm{kJ\ mol^{-1}}$ [48] or $70\ \mathrm{kJ\ mol^{-1}}$ [53]) measurements are more in accordance with the macroscopic activation energy determined by TSDC ($57\ \mathrm{kJ\ mol^{-1}}$) than the one calculated through the IDC data ($40\ \mathrm{kJ\ mol^{-1}}$). Despite these weak differences, we conclude that the results derived from TSDC and IDC data are in good agreement.

When we consider carefully the temperature behavior of the stretched parameter β_{KWW}, we do not conclude on a strict temperature independence of this parameter. Indeed, two different temperature domains in the β_{KWW} behavior are observed.

β_{KWW} is constant and equal to 0.17 between -160 and $-110°\mathrm{C}$ while β_{KWW} remains constant but equal to 0.11 between -100 and $-40°\mathrm{C}$ within the experimental uncertainty. The transition between these two β_{KWW} temperature behaviors occurs over 10° located in the temperature range where the overlapping of the two components, β_2 and β_1, of the secondary relaxation is observed. Then the stretching parameter of the two overlapped processes involved in the secondary β relaxation can be determined from TSDC and IDC data. We assume that the β_2 and β_1 processes are related to the β_{KWW} parameter equal to 0.17 and 0.11, respectively.

We conclude that the two overlapped processes are not Debye processes and the complexity of the β relaxation process of PET arise from an overlapping of the two complex processes characterized by two different coupling parameters. In the framework of the CM, the temperature behavior of β_{KWW} shows a higher degree of the coupling strength in the β_1 process than in the β_2 component.

These observations are in reasonable agreement with the results of Starkweather [48,54] who find activation entropy values in β process far from being close to zero. To analyze the cooperative or the non-cooperative nature of mechanical or dielectric relaxation of polymer, a criterion has been introduced by Starkweather [48,54]. A relaxation is considered simple (non-cooperative) or complex (cooperative) depending on its activation entropy value. Whereas simple relaxations have an activation entropy (ΔS) near zero, complex relaxations present a clear non-zero ΔS value. Starkweather [48,54] has concluded that localized motions involved in the secondary relaxation of PET are performed in a cooperative manner. Since the stretched exponent β_{KWW} of β_1 and β_2 are considerably lower than unity, our results are in agreement with the observations of Starkweather [48,54].

The two components of the β relaxation process are characterized by two different low values of β_{KWW}. Hence molecular motions responsible for the β_1 and β_2 relaxation processes are cooperative in nature but with different degrees of cooperativity as reported by Maxwell et al. [11]. In their recent mechanical investigations, Maxwell et al. [11] show that the high-temperature side of the β mechanical peak of PET is associated with cooperative motions of phenyl rings and the low-temperature side to cooperative motions of carbonyl groups. These results have also been confirmed in a very recent dielectric work through a combined study of the β mode of PET by TSDC and dynamic dielectric spectroscopy [35].

6. Conclusions

The comparison of IDC and TSDC experiments has been shown to be a powerful tool in obtaining consistent information about the dielectric relaxation behavior of amorphous PET, particularly far below the glass transition temperature T_g. The $\beta_{KWW}(T)$ temperature behavior, determined from TSDC spectra obtained at different heating rates and interpreted by the CM, is confirmed by the IDC results. The dynamics of the secondary β relaxation is characterized by a low-temperature independent coupling parameter β_{KWW}.

The different analyses, adopted to determine the stretching parameter β_{KWW} of β relaxation in amorphous PET, provide reliable results and new insights about the cooperative nature of the secondary relaxation of polymers without the side chain.

References

[1] Williams GC, Watts DC. Trans Faraday Soc 1970;66:80.
[2] Havriliak S, Negami S. J Polym Sci C 1966;14:99.
[3] Havriliak S, Negami S. Dielectric and mechanical relaxation in material. Munich: Hanser, 1997.
[4] Alvarez F, Alegria A, Colmenero J. Phys Rev B 1991;44:7306.
[5] Cole KS, Cole RH. J Chem Phys 1941;9:341.
[6] Casalini R, Fioretto D, Livi A, Lucchesi M, Rolla PA. Phys Rev B 1997;56:3016.
[7] Bergmann R, Alvarez F, Alegria A, Colmenero J. J Chem Phys 1998;109:7546.
[8] Bergmann R, Alvarez F, Alegria A, Colmenero J. J Non-Cryst Solids 1998;235–237:580.
[9] Reddish W. Trans Faraday Soc 1949;46:459.
[10] Coburn JC, Boyd H. Macromoecules 1986;19(8):2238.
[11] Maxwell AS, Monnerie L, Ward IM. Polymer 1998;39:6851.
[12] Hofmann A, Kremer F, Fisher EW. Physica A 1993;201:106.
[13] Richert R. Private communication.
[14] Illers KH, Breuer HJ. J Colloid Sci 1963;18:1.
[15] Maxwell AS, Ward IM, Lauprêtre F, Monnerie L. Polymer 1998;39:6835.
[16] Rendell RW, Ngai KL, Mashimo S. J Chem Phys 1987;87:2359.
[17] Alegria A, Guerriera-Echevarria E, Telleria I, Colmenero J. J Phys Rev B 1993;47:14 857.
[18] Alegria A, Guerrica , Echevarria E, Goitiandra L, Telleria I, Colmenero J. Macromolecules 1995;28:1516.
[19] Wagner H, Richert R. Polymer 1997;38:255.
[20] Colmenero J. J Non-Cryst Solids 1991;131–133:860.
[21] Alegria A, Goitiandra L, Colmenero J. Polymer 1996;37:2915.
[22] Alegria A, Goitiandra L, Telleria I, Colmenero J. Macromolecules 1997;30:3881.
[23] Ngai KL, Roland CM. Macromolecules 1993;26:6824.
[24] Alegria A, Santangelo PG, Ngai KL, Roland CM. Macromolecules 1994;27:407.
[25] Roland CM, Santangelo PG, Baram Z, Runt J. Macromolecules 1994;27:5382.
[26] Roland CM. Macromolecules 1995;28:3463.
[27] Ngai KL, Plazek DJ, Rizos AK. J Polym Sci: Polym Phys 1997;35:599.
[28] Ngai KL, Wang CH, Fytas G, Plazek DJ. J Chem Phys 1987;86:4768.
[29] Colmenero J, Arbe A, Alegria A. Phys Rev Lett 1993;71:2603.
[30] Rizos AK, Jian T, Ngai KL. Macromolecules 1995;28:517.
[31] Arbe A, Buchenau U, Willner L, Richter D, Farago B, Colmenero J. J Phys Rev Lett 1996;76:1872.
[32] Richter D, Arbe A, Colmenero J, Monkenbush M, Farago B, Faust R. Macromolecules 1998;31:1133.
[33] Ngai KL, Rendell RW, Yee AF. Macromolecules 1988;21:3396.
[34] Ngai KL, Rendell RW, Yee AF, Plazek DJ. Macromolecules 1991;24:61.
[35] Menegotto J, Demont P, Bernes A, Lacabanne C. J Polym Sci, Part B: Polym Phys 1999;37(24):3494–503.
[36] Ngai KL. Comments Solid State Phys 1980;9:127.
[37] Ngai KL. Comments Solid State Phys 1979;9:141.
[38] Ngai KL, Rendell RW, Rajagopal AK, Teitler S. Ann N Y Acad Sci 1986;484:150–84.
[39] Ngai KL, Tsang K. Macromol Symp 1995;90:95.
[40] Ngai KL. In: Richert R, Blumen A, editors. Disorder effects on relaxation processes — glasses, polymers, protein. Berlin: Springer, 1994.
[41] Marchal E. J Chem Phys 1992;96:4676.
[42] Marchal E. Makromol Chem Rapid Commun 1993;14:597.
[43] Marchal E. J Non-Cryst Solids 1994;172–174:902.
[44] Marchal E. J Chem Phys 1996;105:6068.
[45] Bucci C, Fieschi R. Phys Rev Lett 1964;12:16.
[46] Teyssedre G, Mezghani S, Bernes A, Lacabanne C. In: Runt JP, Fitzgerald AM, editors. Dielectric spectroscopy of polymeric materials. Washington, DC: American Chemical Society, 1997.
[47] Menegotto J, Ibos L, Bernes A, Demont P, Lacabanne C. Ferroelectrics 1999;228:1.
[48] Starkweather HW. Macromolecules 1990;23:328.
[49] Bernes A, Chatain D, Lacabanne C. IEEE Trans Electr Insul 1992;27:3.
[50] Dargent E, Santais JJ, Saiter JM, Bayard J, Grenet J. J Non-Cryst Solids 1994;172–174:1062.
[51] Van Turnhout J. Thermally stimulated discharge of polymers electrets. Amsterdam: Elsevier, 1975.
[52] Hofmann A, Kremer F, Fisher EW, Schonhals A. In: Richert R, Blumen A, editors. Disorder effects on relaxation processes — glasses, polymers, proteins. Berlin: Springer, 1994.
[53] Perez J, Cavaillé JY. J Phys III France 1995;5:79.
[54] Starkweather HW. Macromolecules 1981;14:1277.